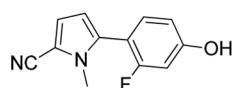


# Structure-Based Approach To Identify 5-[4-Hydroxyphenyl]pyrrole-2-carbonitrile Derivatives as Potent and Tissue Selective Androgen Receptor Modulators

Ray Unwalla,\*<sup>1b</sup> James J. Mousseau, Olugbeminiyi O. Fadeyi,<sup>1b</sup> Chulho Choi, Kevin Parris, Baihua Hu, Thomas Kenney, Susan Chippari, Christopher McNally, Karthick Vishwanathan, Edward Kilbourne, Catherine Thompson, Sunil Nagpal, Jay Wrobel, Matthew Yudt, Carl A. Morris, Dennis Powell, Adam M. Gilbert, and Eugene L. Piatnitski Chekler\*

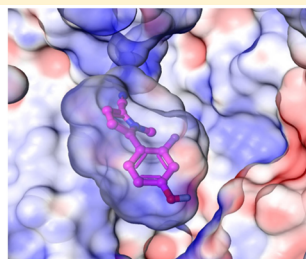
Pfizer Worldwide Research & Development, 610 Main Street, Cambridge, Massachusetts 02139, United States

## S Supporting Information



Compound 7

ARE-LUC  $EC_{50}$  = 0.34 nM (81 %Eff)  
N/C Interaction  $EC_{50}$  = 1206 nM (46 %Eff)



**ABSTRACT:** In an effort to find new and safer treatments for osteoporosis and frailty, we describe a novel series of selective androgen receptor modulators (SARMs). Using a structure-based approach, we identified compound 7, a potent AR (ARE  $EC_{50}$  = 0.34 nM) and selective (N/C interaction  $EC_{50}$  = 1206 nM) modulator. In vivo data, an AR LBD X-ray structure of 7, and further insights from modeling studies of ligand receptor interactions are also presented.

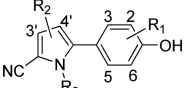
## INTRODUCTION

The steroids testosterone and dihydrotestosterone (DHT) are androgens that play an important role in the development and maintenance of a variety of physiological responses such as male sexual function, bone density, muscle mass, and strength.<sup>1</sup> The androgen receptor is a nuclear hormone receptor that is expressed in many tissues and is responsible for mediating the actions of testosterone and DHT. Patients that have defects in the androgen receptor or have androgen deficiencies can be effectively treated with exogenous testosterone and other steroidal androgens as a hormone replacement therapy.<sup>2–4</sup> The anabolic effects of testosterone have shown benefit in age-related decline of bone density and muscle mass.<sup>5</sup> However, the side-effect profile of testosterone and other currently available anabolic steroids precludes their widespread use, and the chronic administration of steroidal androgens is associated with potential serious side effects such as hepatotoxicity, prostate hypertrophy, and cancer. In addition, the oral bioavailability of testosterone is poor and the route of its administration is generally through topical formulations. As a result, several companies have undertaken efforts to find nonsteroidal selective androgen receptor modulators (SARMs) that exhibit desired anabolic effects but are devoid of androgenic effects.

In the estrogen field, the development of tissue-selective estrogen receptor modulators (SERMs) for the prevention and treatment of postmenopausal osteoporosis has provided the

proof-of-concept that nonsteroidal compounds have the potential to function as an agonist in one tissue and an antagonist in another.<sup>6</sup> Researchers in the androgen field have used the lessons learned from the SERM field to develop SARMs for the treatment of male and female osteoporosis and frailty. This new second generation of nonsteroidal SARMs includes BMS-564929 (Bristol-Myers Squibb Co),<sup>7</sup> ostarine (GTx Inc.),<sup>8</sup> and MK-0773 (Merck & Co)<sup>9</sup> (Figure S1 in Supporting Information). These SARMs exhibited tissue-selective profiles in preclinical studies, indicating that they may provide the required tissue selectivity for a muscle selective agent.<sup>10</sup> However, the clinical utility of oral SARMs appears to be limited due to the unfavorable plasma lipoprotein changes such as lowering of HDL-C<sup>11a</sup> which results in the increased risk of cardiovascular diseases. It has been reported that decreased plasma HDL-C levels are due to liver mediated effects of AR activation. Current testosterone replacement therapies have focused on use of topical formulations to minimize these lipid changes and hepatic side effects. There are also recent reports of transdermal SARMs for the treatment of various muscles wasting disorders that potentially mitigate CV and prostate risk.<sup>11b,c</sup> We have previously reported SARM series that selectively affect the muscle tissue versus the

Received: March 15, 2017

Table 1. Structure–Activity Relationship of *N*-Me Pyrrole Derivatives 1–25<sup>a</sup>


compd	R <sub>1</sub>	R <sub>2</sub>	R <sub>3</sub>	ARE-LUC agonist, EC <sub>50</sub> (nM) (% efficacy)	binding, IC <sub>50</sub> (nM)	N/C interaction, EC <sub>50</sub> (nM) (% efficacy)
1	2,3-cyclopentyl	H	Me	17.8 (85)	8.1	>10000
2	H	H	Me	573.2 (103)	6.3	2014.9 (36)
3	2-Me	H	Me	37.3 (91)	2.9	1542.6 (42)
4	3-Me	H	Me	94.8 (69)	3.7	1550.9 (37)
5	2-Et	H	Me	391.0 (74)	7.1	>10000
6	2-F	H	Me	1517.7 (69)	59.0	>10000
7	3-F	H	Me	0.34 (91)	3.2	1205.8 (46)
8	2-Cl	H	Me	909.5 (80)	47.6	>10000
9	3-Cl	H	Me	1.7 (80)	1.4	1556.0 (31)
10	3-CF <sub>3</sub>	H	Me	15.2 (69)	14.8	>10000
11	3-NO <sub>2</sub>	H	Me	233 (77)	65.0	>10000
12	3-CN	H	Me	29.7 (82)	6.8	>10000
13	3-COOMe	H	Me	1450.3 (36)	330.2	>10000
14	3-SO <sub>2</sub> Me	H	Me	>10000	1465.9	>10000
15	3,5-di-F	H	Me	0.14 (90)	1.6	0.71 (61)
16	3,6-di-F	H	Me	229.1 (84)	85.8	>10000
17	2,3-di-F	H	Me	980.0 (85)	36.8	>10000
18	3-F, 5-CN	H	Me	5.3 (112)	67.4	28.9 (49)
19	3,5-di-Cl	H	Me	0.17 (76)	28.7	>10000
20	2,3-di-Me	H	Me	34.6 (116)	4.9	>10000
21	H	4'-Br	Me	1644.6 (31)	166.9	>10000
22	H	3'-CF <sub>3</sub>	Me	1341.7 (66)	11.1	>10000
23	3-F	H	Et	1136.4 (64)	127.1	>10000
24	3-F	H	CH <sub>2</sub> CN	>10000	6032.0	>10000
25	3-F	H	CH <sub>2</sub> COOH	>10000	>10000	>10000

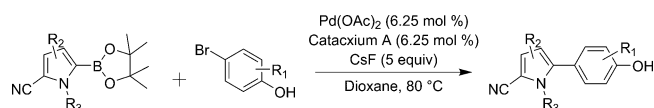
<sup>a</sup>Values are the geometric mean of at least three experiments. If % efficacy or % inhibition is <30%, EC<sub>50</sub> and IC<sub>50</sub> of >10000 nM are reported.

prostate.<sup>12</sup> These compounds show diminished activity in promoting the intramolecular interaction between the AR carboxyl (C) and amino (N) termini in an N/C-termini interaction assay. This assay has been reported previously by Ghali et al.<sup>13</sup> and has been shown to be a good predictor for undesired androgenic responses in vivo. Thus, a desired profile for a muscle selective AR modulator would be to have minimal activity in the N/C-interaction assay. The following report outlines our strategy to identify and optimize a series of functionally selective 5-(4-hydroxyphenyl)pyrrole-2-carbonitriles using a structure-based design/docking approach that maintains favorable in vitro and in vivo profile on muscle tissue with minimum effects on the prostate.

## RESULTS AND DISCUSSION

In our effort to design novel AR inhibitors, we utilized a cyanopyrrole scaffold discovered in the course of a high-throughput screening campaign of our corporate library. The in vitro profile of **1** (Table 1), 5-(7-hydroxy-2,3-dihydro-1*H*-inden-4-yl)-1-methylpyrrole-2-carbonitrile, encouraged us to conduct further structure–activity studies to improve potency and physicochemical properties. 5-(4-Hydroxyphenyl)-1-methylpyrrole-2-carbonitrile SARMs (**2–25** in Scheme 1) were prepared via Suzuki cross-coupling of 4-OH-aryl bromides with 2-pyrrolboronates (Scheme 1).<sup>14</sup> Boronic acids were commercially available or prepared according to published procedures described in the Supporting Information (experimental and analytical information for **1–6**, and **8–25** is presented in the Supporting Information).

### Scheme 1. Preparation of 5-(4-Hydroxyphenyl)-1-methylpyrrole-2-carbonitriles



**Structure–Activity Relationships.** The in vitro anabolic activity was assessed in androgen response element luciferase (ARE-LUC) assay in CV-1 cells. Agonism in this assay is predictive of in vivo muscle activity. The androgenic activity was measured using the N/C-interaction in CV-1 cells. A radiolabeled AR ligand binding assay was performed using [<sup>3</sup>H]mibolerone in COS cells transfected with the AR. Table 1 shows the results of the ARE-LUC, AR binding, and N/C-interaction functional assays. The project strategy was to select compounds with minimal activity in N/C-interaction assay relative to the ARE-LUC assay for advancement into in vivo assessment. Thus, maintaining the agonism to support the muscle growth and reducing the androgenic effect (N/C-interaction) should result in tissue selective compounds.

Compound **1** was used as a starting point in a search for tissue selective compounds. To delineate the critical structural features responsible for the binding, we performed docking studies on **1** with X-ray structure of published AR ligand binding domain (LBD) (PDB code 2AXA).<sup>15</sup> The top-scoring pose<sup>16</sup> from docking showed the nitrile group of the pyrrole ring forming a hydrogen bond with Arg752 residue. The amino group of Gln711 residue was in a nearby position to the nitrile

group to form a hydrogen bond, but the angle was found to be not optimal for such an interaction. The hydroxyl group of the phenol formed a hydrogen bond with the carbonyl group of the Asn705 residue. The *N*-methyl group was oriented toward helix-3 and was surrounded by residues Leu704 and Leu707, whereas the fused cyclopentyl ring of **1** was oriented toward the pocket surrounded by the hydrophobic residues Met780 and Phe764, as shown in (Figure S2). Recognizing that the hydroxyl and nitrile groups were critical for hydrogen bonding with the AR receptor, we decided to keep those features and optimize the rest of the core scaffold. Throughout our optimization processes we noticed that subtle changes on the ligand scaffold had a substantial effect on the functional activity. This type of behavior, whereby small structural changes on the ligand modulate functional activity has been previously observed with other nuclear receptors such as progesterone.<sup>17</sup> Removal of the fused cyclopentyl ring (i.e., **2**) surprisingly did not result in any loss of binding ( $IC_{50}$  (binding) of  $\sim 6.3$  nM vs 8.1 nM), but it did reduce agonist activity. This observation became the first indication that the binding and the functional potencies do not perfectly correlate ( $R^2 \approx 0.5$ ). This phenomenon supports a general hypothesis that the functional activity is an outcome of a complex process of cofactors binding to the AR termini and may not be directly proportional to binding affinity.<sup>12</sup> As this phenomenon deserves a further investigation, the team proceeded to optimize in vitro profile based on functional activity. However, the binding potency remained an important indicator of the ligand–receptor interactions, and a general trend was observed that a low nM binding potency is required to achieve functional activity although not every potent binder became a strong agonist (Table 1). The potency of **2** was encouraging, and this template provided us further exploration of the 3 and 5 positions of the phenol scaffold.

Compound **7** activity in the ARE-LUC assay approaches the potency of testosterone in the same assay ( $EC_{50} \approx 0.3$  nM), while the activity in N/C-interaction assay provided more than a 4000-fold selectivity window between in vitro anabolic and androgenic predictive assays (Figure S3). Compound **7** became a lead molecule for proof-of-concept studies for both in vitro and in vivo assays. The SAR around **7** first demonstrates that groups in the 3-position (**7** and **9**) are preferred to analogs substituted in the 2-position (**6** and **8**). Larger groups in the 3-position (**10–14**) exhibited partial or complete loss of functional activity and a loss in binding affinity. This outcome can be rationalized by a relatively small size of the binding area around the phenyl ring. The preferred 3-position inspired an additional exploration of the chemical space where disubstituted analogs **15–20** were prepared. Substitution at the 3 or at both 3 and 5 positions with small electron withdrawing groups proved to be most fruitful for activity and pushed these compounds into desirable lipophilic ligand efficiency (LipE) space of  $>5$  (for a discussion on the LipE parameter that combines potency and lipophilicity parameters of ligands, see Supporting Information Figure S4). The 3,5-difluoro compound **15** demonstrated superior agonist potency compared to **7**, but the activity in N/C-interaction assay increased dramatically (Table 1). The reason for the switch in the balance of ARE-LUC and N/C-interaction potencies remains highly elusive with minor changes in structure leading to significant functional activity profile changes. This phenomenon has been discussed previously.<sup>12</sup> A general trend exists that all compounds potent in N/C-interaction assay also demonstrate the agonist activity in the ARE-LUC assay. We also explored

other regions of the phenylpyrrole scaffold in a search for additional switch points of functional activity. Substitution on the pyrrole in **21** and **22** led to the loss of potency compared to **2**. That the *N*-methyl group of pyrrole is the optimal substituent is shown by analogs **23–25**. A number of previously published derivatives<sup>14</sup> where phenolic group was replaced with an amine were also tested in the ARE-LUC and binding assays, but no potent and selective compounds were discovered (see Supporting Information).

Compound **7** showed a unique biological profile compared to endogenous AR agonists such as testosterone and DHT. While both testosterone and **7** are potent in ARE-LUC assay, only testosterone shows potent N/C-interaction activity ( $EC_{50} = 1.1$  nM, Figure S3). Also, the lead molecule **7** demonstrated greater than 1000-fold selectivity against a panel of nuclear receptors including progesterone receptor where only weak agonist activity (54% at  $10 \mu\text{M}$ ) was observed in a PRE assay which is equivalent to the ARE assay. In addition to the data presented above, the 5-(4-hydroxyphenyl)-1-methylpyrrole-2-carbonitriles showed no activity in hERG dofetilide binding assay with  $IC_{50} > 100 \mu\text{M}$  for **7** and no effect on proliferation ( $IC_{50} > 300 \mu\text{M}$ ) in the human liver cell line (THLE). There was also no significant inhibition of cytochrome P450 enzymes CYP3A4, CYP2C9, CYP2D6, CYP1A2, and CYP2C8 at  $3 \mu\text{M}$  compound concentration. Additionally, no in-life toxicological effects were observed for **7** when tested in vivo.

**Molecular Modeling and Crystallography.** We later determined the X-ray crystal structure of **7** bound to the AR LBD at a resolution of  $2.3 \text{ \AA}$ , as shown in Figure 1. As expected

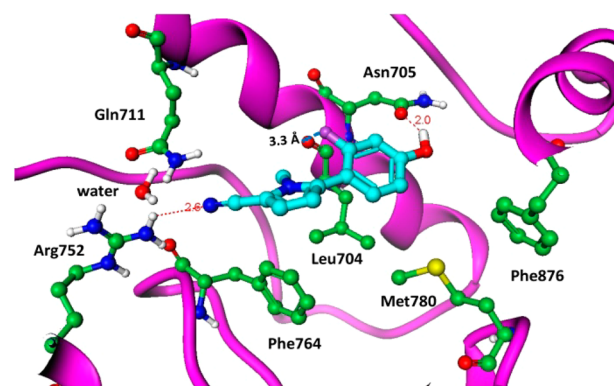


**Figure 1.** X-ray structure of **7** (PDB code 5V04) in the AR ligand binding domain. Ligand is colored in cyan, and the critical residues are shown in green. Hydrogen bond distances are shown by red dotted lines in  $\text{\AA}$ . The distance between the fluoro group and the carbonyl backbone of residues Leu704, i.e.,  $3.3 \text{ \AA}$ , is shown by dotted blue line.

from our docking studies, the observed binding mode was similar to the docked pose of **1**, the nitrile group formed critical hydrogen bond with the Arg752 residue, whereas the phenolic hydroxyl group had a hydrogen bond with the Asn705 side chain. A highly ordered water molecule was present between the Arg752 and Gln711 residues which is reminiscent of a similar network observed in the LBD of the progesterone receptor.<sup>18</sup> The dihedral angle of  $47^\circ$  between the phenol and the cyanopyrrole group provided an optimal orientation for the ligand to ensure that key hydrogen bond interactions are achieved within the binding pocket. The position of 3-fluoro group of the ligand near the Leu704 residue of the binding site was especially surprising since the atom closest to the fluorine

was the oxygen of the carbonyl backbone of the Leu704 residue, at a distance of 3.3 Å between the oxygen and fluorine atoms. The bond dipoles (i.e., the C(Ar)–F and C(=O) groups) were oriented in parallel and the angle between dipoles was  $\sim 23^\circ$  as shown in Figure 1. The orientation of the fluorine atom close to the oxygen atom would indicate an unfavorable electrostatic interaction for the ligand, so we examined the unbiased electron density difference maps of the ligand in order to confirm the fluorine atom orientation. The maps showed that there was a clear density for the placement of the fluorine atom near the carbonyl backbone of the Leu704 residue. There was no other density within the binding site to suggest an alternative location for the fluorine atom (Figure S5A). The mining of the Cambridge Structural Database<sup>19</sup> and the Protein Data Bank showed several examples of a fluorine atom being in close contact with a carbonyl group, i.e., distance (C–F...C(=O)) of approximately 3.0–3.8 Å) in small and large molecule X-ray structures. However, in these cases the preferred approach of the fluorine atom is toward the carbonyl carbon in an orthogonal orientation (e.g., at an angle  $\sim 170$ – $180^\circ$  in C–F–C(=O)); see Figure S5B). A recent study demonstrated that these interactions are favorable in protein–ligand X-ray structures and may help to increase the potency of inhibitors.<sup>20</sup> The parallel orientation of the two bond dipoles in our crystal structure was surprising because this type of dipole–dipole interaction leads to weak but still unfavorable electrostatic interactions. The magnitude of such an interaction is unclear, particularly given the specific protein–ligand contacts we observed in the X-ray structure. To understand the energetics of the ligand-bound conformation of 7, we calculated the local and global ligand strain energies. The local strain energy is the energy difference between the ligand-bound conformation and its nearest local minimum conformation in the unbound state, while the global strain energy is difference between the energies of the ligand-bound state conformation and the global minima conformation of the unbound ligand.

Both local and global strain energy calculations using two widely used molecular mechanics force fields (MMFF94 and OPLS2005) confirm that 7 pays only a small energy penalty for the bound state: a mean local strain energy of 0.33 kcal/mol and a mean global strain energy of 0.54 kcal/mol (Table S1). These energies are well below the threshold established for the local and global strain energies for a ligand with 1–3 rotatable bonds found in a benchmark study of 150 X-ray structures of protein–ligand complexes.<sup>21</sup>

The interaction of 3-fluoro group with the carbonyl backbone of Leu704 was further examined by calculating the intermolecular potential between these groups. To provide valuable insights into the strength of such an interaction, we used a model system between a 3-fluorophenol group (representative of 7) and the carbonyl backbone of leucine modeled as *N*-methylacetamide and performed ab initio quantum chemical calculations. Figure S6A shows the potential energy<sup>22a</sup> of 3-fluorophenol varies as a function of distance from *N*-methylacetamide (a model for the backbone carbonyl group). When fluorine approaches the oxygen of the carbonyl group atom, the interaction is indeed repulsive as we had expected; however, the magnitude of the repulsive interaction at the X-ray observed distance of  $\sim 3.3$  Å is only  $\sim 0.6$  kcal/mol. Thus, there are two factors at play when the ligand adopts the bound state conformation. The low strain energy of the ligand along with a favored torsion profile<sup>22b</sup> (Figure S6B) in the bound state allows the ligand to bind in a similar conformation

as found in the unbound state and to be able to compensate for the small unfavorable electrostatic interaction, i.e.,  $\sim 0.6$  kcal/mol of the 3-fluoro group with the carbonyl backbone of Leu704 residue.

**Pharmacokinetics.** Compound 7 was selected based on its potent agonist activity in the ARE-LUC assay, minimal activity in the N/C-interaction assay, and good physicochemical and ADME properties (cLogP = 2.6; solubility at pH 6.5, 146  $\mu$ M; human liver microsomal clearance, 40  $\mu$ L min<sup>-1</sup> mg<sup>-1</sup>; passive permeability RRCK cell line  $P_{app}(AB) = 29 \times 10^{-6}$  cm/s; Pgp influenced efflux in MDR cells, ratio BA/AB = 2). The pharmacokinetic (PK) studies of 7 in rats (Table 2) reveal that

**Table 2. Pharmacokinetic Parameters for 7 in Rats**

parameter	route		
	2 mg/kg, iv	10 mg/kg, ip	10 mg/kg, po
Clp (mL min <sup>-1</sup> kg <sup>-1</sup> )	35		
$V_{ss}$ (L/kg)	0.5		
AUC (ng·h/mL)	970	2492	421
$T_{1/2}$ (h)	0.4	1	1
$C_{max}$ (ng/mL)		2617	110
$T_{max}$ (h)		1	2
$F$ (%)		51	9

the intraperitoneal (ip) route achieved a robust maximum concentration, a fast onset of  $C_{max}$  and a good availability when compared to oral (po) or intravenous (iv) PK. Thus, the decision was made to proceed with proof-of-concept in vivo efficacy studies via ip route of administration.

**In Vivo Studies.** Compound 7 was evaluated in 4-day immature orchidectomized rats that lack endogenous testosterone production and are expected to have an exaggerated effect upon treatment with exogenous androgens. The levator ani muscle is the most androgen-sensitive muscle in orchidectomized rats. Testosterone propionate (TP) was expected to have an effect on muscle and reproductive system organs. After the compound administration the weights of prostate, seminal vesicles, and levator ani muscle tissues were measured and compared with the organ weights of vehicle-treated animals and the testosterone-treated group. The effects of 1, 3, 10, and 30 mg/kg doses of 7 are shown in Figure 2. The ip administration of 7 showed a statistically significant increase in the levator ani muscle weight at 10 and 30 mg/kg. Importantly, 7 did not show increase in weights for the ventral prostate and seminal vesicles over the vehicle-treated group except for a small but statistically significant increase in the 30 mg/kg group.

As a positive control, TP promoted anabolic and androgenic responses in this model and induced significant tissue weight changes in seminal vesicles, prostate, and levator ani muscle when administered at 1 mg/kg sc once daily. This study suggests that at least at 10 mg/kg dose 7 elicits an anabolic effect on muscle mass while showing no androgenic effects. Compound 7 demonstrated a therapeutic index with respect to separation of anabolic and androgenic activities. We also found that the concentrations of 7 in muscle, prostate, and seminal vesicles were similar (data not shown), thereby indicating that the observed tissue selectivity effects are not due to differences in compound distribution between these tissues.

Hypothalamus–pituitary–gonadal axis, or HPG axis, is the main regulating mechanism for testosterone level.<sup>23</sup> The anterior portion of the pituitary gland produces luteinizing

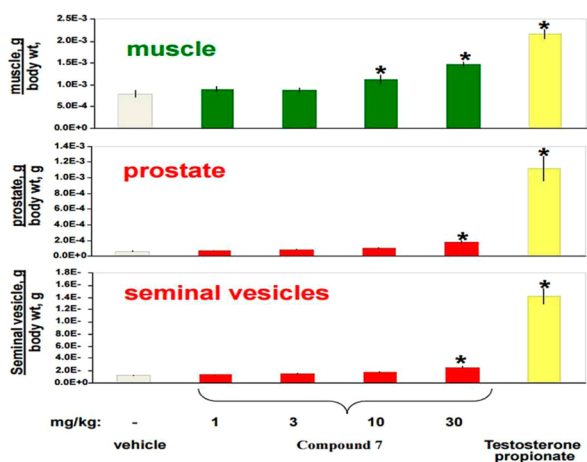


**Figure 2.** Effects of 1, 3, 10, or 30 mg/kg on ip administration of 7 on the tissue weights of seminal vesicles, prostate, and levator ani muscle in orchidectomized male rats ( $(*) p < 0.05$  vs vehicle). TP was dosed at 1 mg/kg sc.

hormone (LH) which is a key regulator for testosterone production in the body. Once levels of testosterone become elevated, additional testosterone production is suppressed via LH regulation through a negative feedback effect on the pituitary gland (Figure 3A). Unlike exogenous androgens that

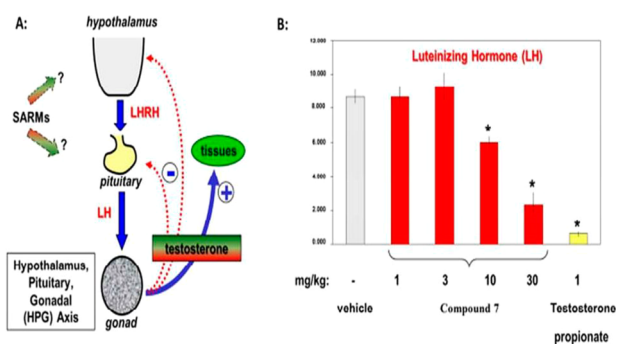


**Figure 3.** (A) Hypothalamus–pituitary–gonadal (HPG) axis is the main regulating mechanism for testosterone level. (B) Effects of 1, 3, 10, or 30 mg/kg on ip administration of 7 on luteinizing hormone concentrations in orchidectomized male rats ( $(*) p < 0.05$  vs vehicle). TP was dosed at 1 mg/kg sc.

suppress LH release substantially, an ideal SARM would show a reduced LH suppression and a minimum effect on the testosterone production. Compound 7 effect on LH levels was evaluated in the course of exploratory 14-day toxicology study. At 10 mg/kg, a decrease in LH levels was observed which was statistically significant and the 30 mg/kg dose led to a substantially lower concentration of LH compared to a vehicle-treated group (Figure 3B). As expected, TP at 1 mg/kg SC produced significantly reduced LH levels. Therefore, 7 is recognized as an androgen receptor binder in the brain that leads to a decrease in endogenous testosterone/LH levels in rats which may or may not translate to humans. However, our preclinical models cannot be used to establish a window with respect to testosterone lowering in humans. Testosterone levels and regulation are highly species dependent, also with a huge variability within the same species. Testosterone levels in animals are highly dependent on social organization.

## CONCLUSIONS

Herein, we have detailed the synthesis and biological activity of a novel series of tissue-selective androgen receptor modulators (SARMs), i.e., cyanopyrroles that selectively promote muscle growth while showing reduced androgenic effects on the prostate and seminal vesicles. Our SAR efforts using a combined structure-based and docking approach led to a putative binding mode of the ligand which allowed further optimization of this series. We utilized the anabolic ARE-LUC and the androgenic N/C-terminal interaction in vitro assays to identify compounds that show tissue selectivity effects in vivo. By using this strategy, we were able to identify lead compound 7, a potent SARM molecule that is in good physicochemical property space (i.e.,  $MW \approx 216$ ;  $cLogP \leq 3$ ) and shows a good separation of anabolic (ARE  $EC_{50} = 0.34$  nM) and androgenic activities (N/C-interaction  $EC_{50} = 1206$  nM). In a 4-day immature orchidectomized rat in vivo model, 7 significantly increased levator ani muscle growth at the two highest doses 10 and 30 mg/kg and demonstrated selectivity over seminal vesicle and prostate tissues at least at one of the doses, i.e., 10 mg/kg. These data suggest 7 would be a valuable tool molecule for further evaluation and comparison to other SARMs in clinical trials. Our ongoing efforts toward these objectives will be described in future publications. An AR LBD X-ray structure of 7 offered useful insights on ligand strain energy and the nature of ligand–receptor interactions.

## EXPERIMENTAL SECTION

**General Experiment. General Procedure for Suzuki Coupling (Scheme 1).** All solvents/water were degassed with inert atmosphere for 30 min prior to use. To a 60 mL sealed tube with stir bar was added the boronate (1.5 equiv), bromide (1 equiv),  $Pd(OAc)_2$  (6.25 mol %), and cataclium A (6.25 mol %). The vial was sealed and sparged with argon. Degassed dioxane (0.05 M) was added under argon flow followed by CsF solution (5.1 equiv, 1 M in degassed water, solution prepared under argon atmosphere). The mixture was stirred at 80 °C for 1 h at which time the reaction was determined to be complete. The resulting solution was cooled to room temperature, filtered through Celite, concentrated under reduced pressure, and purified by automated preparatory SFC. All compounds used in this study (Table 1) were characterized with  $^1H$  and  $^{13}C$  NMR spectroscopy, ESI-MS, and HPLC. The purities of all final compounds were confirmed to be  $\geq 95\%$  by high-performance liquid chromatography (HPLC). All data for compound characterization are provided in Supporting Information.

**Preparation of 5-(2-Fluoro-4-hydroxyphenyl)-1-methyl-1H-pyrrole-2-carbonitrile (7).** The title compound was prepared according to the general procedure using 0.578 mmol of 4-bromo-3-fluorophenol and 0.607 mmol of 1-methyl-5-(4,4,5,5-tetramethyl-1,3,2-dioxaborolan-2-yl)-1H-pyrrole-2-carbonitrile. The product was purified by prep SFC ( $dC_{18}$  5  $\mu m$ , 4.6 mm  $\times$  50 mm, EtOH, 2 mL/min, retention time 2.7021 min) to give 65 mg of a yellow solid (51% yield).  $^1H$  NMR (500 MHz, DMSO)  $\delta$  10.38 (br s, 1H), 7.22–7.27 (m, 1H), 7.01 (d,  $J = 4.16$  Hz, 1H), 6.68–6.74 (m, 2H), 6.23 (d,  $J = 3.91$  Hz, 1H), 3.56 (d,  $J = 1.22$  Hz, 3H).  $^{13}C$  NMR (126 MHz, DMSO)  $\delta$  159.4, 158.6, 158.5, 157.4, 132.4, 130.9, 130.9, 117.8, 112.4, 110.5, 110.5, 108.9, 107.1, 107.0, 102.5, 101.4, 101.2, 31.7, 31.7. HRMS calcd for  $C_{12}H_{10}FN_2O$  ( $M + H$ ) $^+$ : 217.0772. Found: 217.0774.

## ASSOCIATED CONTENT

### Supporting Information

The Supporting Information is available free of charge on the ACS Publications website at DOI: 10.1021/acs.jmedchem.7b00373.

Additional information on synthesis procedure and compound characterization; detailed biological assays; figures and tables; X-ray coordinates (PDF)  
Molecular formula strings and some data (CSV)

### Accession Codes

Atomic coordinates for the X-ray structure of **7** can be accessed using PDB code 5V04 in the RCSB Protein Data Bank ([www.rcsb.org](http://www.rcsb.org)). Authors will release coordinates upon article publication.

### AUTHOR INFORMATION

#### Corresponding Authors

\*R.U.: phone, +1-617-674-7398; e-mail, [ray.unwalla@pfizer.com](mailto:ray.unwalla@pfizer.com).

\*E.L.P.C.: phone, +1-718-473-5557; e-mail, [piatnits@gmail.com](mailto:piatnits@gmail.com).

#### ORCID

Ray Unwalla: 0000-0002-5789-7336

Olugbeminiyi O. Fadeyi: 0000-0002-5525-1304

#### Notes

The authors declare no competing financial interest.

### ABBREVIATIONS USED

SARM, selective androgen receptor modulator; AR, androgen receptor; LBD, ligand binding domain; SERM, tissue-selective estrogen receptor modulator; HDL-C, high density lipoprotein cholesterol; LipE, lipophilic ligand efficiency

### REFERENCES

- (1) Mangelsdorf, D. J.; Thummel, C.; Beato, M.; Herrlich, P.; Schutz, G.; Umesono, K.; Blumberg, B.; Kastner, P.; Mark, M.; Chambon, P.; Evans, R. M. The nuclear receptor superfamily: The second decade. *Cell* **1995**, *83*, 835–839.
- (2) Bhasin, S.; Woodhouse, L.; Casaburi, R.; Singh, A. B.; Mac, R. P.; Lee, M.; Yarasheski, K. E.; Sinha-Hikim, I.; Dzekov, C.; Dzekov, J.; Magliano, L.; Storer, T. W. Older men are as responsive as young men to the anabolic effects of graded doses of testosterone on the skeletal muscle. *J. Clin. Endocrinol. Metab.* **2005**, *90*, 678–688.
- (3) Snyder, P.; Peachey, H.; Hannoush, P.; Berlin, J. A.; Loh, L.; Holmes, J. H.; Dlewati, A.; Staley, J.; Santanna, J.; Kapoor, S. C.; Attie, M. F.; Haddad, J. G., Jr.; Strom, B. L. Effect of testosterone treatment on bone mineral density in men over 65 years of age. *J. Clin. Endocrinol. Metab.* **1999**, *84*, 1966–1972.
- (4) Snyder, P. J.; Peachey, H.; Hannoush, P.; Berlin, J. A.; Loh, L.; Lenrow, D. A.; Holmes, J. H.; Dlewati, A.; Santanna, J.; Rosen, C. J.; Strom, B. L. Effect of testosterone treatment on body composition and muscle strength in men over 65 years of age. *J. Clin. Endocrinol. Metab.* **1999**, *84*, 2647–2653.
- (5) Bagatell, C. J.; Bremner, W. J. Androgens in men—uses and abuses. *N. Engl. J. Med.* **1996**, *334*, 707–715.
- (6) Bhavnani, B. R.; Woolever, C. A. Interaction of ring B unsaturated estrogens with estrogen receptors of human endometrium and rat uterus. *Steroids* **1991**, *56*, 201–210.
- (7) Nirschl, A. A.; Zou, Y.; Krystek, S. R.; Sutton, J. C.; Simpkins, L. M.; Lupisella, J. A.; Kuhns, J. E.; Seethala, R.; Golla, R.; Slep, P. G.; Beehler, B. C.; Grover, G. J.; Egan, D.; Fura, A.; Vyas, V. P.; Li, Y.-X.; Sack, J. S.; Kish, K. F.; An, Y.; Bryson, J. A.; Gougoutas, J. Z.; DiMarco, J.; Zahler, R.; Ostrowski, J.; Hamann, L. G. N-Aryl-oxazolidin-2-imine muscle selective androgen receptor modulators enhance potency through pharmacophore reorientation. *J. Med. Chem.* **2009**, *52*, 2794–2798.
- (8) Jones, A.; Hwang, D. J.; Duke, C. B., III; He, Y.; Siddam, A.; Miller, D. D.; Dalton, J. T. Nonsteroidal selective androgen receptor modulators enhance female sexual motivation. *J. Pharmacol. Exp. Ther.* **2010**, *334*, 439–448.

(9) Schmidt, A.; Kimmel, D. B.; Bai, C.; Scafonas, A.; Rutledge, S.; Vogel, R. L.; McElwee-Witmer, S.; Chen, F.; Nantermet, P. V.; Kasparcova, V.; Leu, C.-T.; Zhang, H.-Z.; Duggan, M. E.; Gentile, M. A.; Hodor, P.; Pennypacker, B.; Masarachia, P.; Opas, E. E.; Adamski, S. A.; Cusick, T. E.; Wang, J.; Mitchell, H. J.; Kim, Y.; Prueksaritanont, T.; Perkins, J. J.; Meissner, R. S.; Hartman, G. D.; Freedman, L. P.; Harada, S.-i.; Ray, W. J. Discovery of the selective androgen receptor modulator MK-0773 using a rational development strategy based on differential transcriptional requirements for androgenic anabolism versus reproductive physiology. *J. Biol. Chem.* **2010**, *285*, 17054–17064.

(10) Kilbourne, E.; Moore, W.; Freedman, L.; Nagpal, S. Selective androgen receptors modulators for frailty and osteoporosis. *Curr. Opin. Invest. Drugs* **2007**, *8*, 821–829.

(11) (a) Schleich, F.; Legros, J. Effects of androgen substitution on lipid profile in the adult and aging hypogonadal male. *Eur. J. Endocrinol.* **2004**, *151*, 415–424. (b) Saeed, A.; Vaught, G.; Gavardinas, K.; Matthews, D.; Green, J. E.; Losada, P.; Bullock, H.; Calvert, N.; Patel, N.; Sweetana, V.; Krishnan, V.; Henck, J.; Luz, J.; Wang, Y.; Jadhav, J. 2-Chloro-4-[(1R,2R)-2-hydroxy-2-methylcyclopentyl]amino]-3-methyl-benzonitrile: A transdermal selective androgen receptor modulator (SARM) for muscle atrophy. *J. Med. Chem.* **2016**, *59*, 750–755. (c) Ullrich, T.; Sasmal, S.; Boorgu, V.; Pasagadi, S.; Cheera, S.; Rajagopalan, S.; Bhumireddy, A.; Shashikumar, D.; Chelur, S.; Belliappa, C.; Pandit, C.; Krishnamurthy, N.; Mukherjee, S.; Ramanathan, A.; Ghadiyaram, C.; Ramachandra, M.; Santos, P.; Lagu, B.; Bock, M.; Perrone, M.; Weiler, S.; Keller, H. 3-Alkoxy-pyrrolo[1,2-b]pyrazolines as selective androgen receptor modulators with ideal physicochemical properties for transdermal administration. *J. Med. Chem.* **2014**, *57*, 7396–7411.

(12) Chekler, E. L. P.; Unwalla, R.; Khan, T. A.; Tangirala, R. S.; Johnson, M.; St. Andre, M.; Anderson, J. T.; Kenney, T.; Chiparri, S.; McNally, C.; Kilbourne, E.; Thompson, C.; Nagpal, S.; Weber, G. L.; Schelling, S.; Owens, J.; Morris, C. A.; Powell, D.; Verhoest, P. R.; Gilbert, A. M. 1-(2-Hydroxy-2-methyl-3-phenoxypropionyl)indoline-4-carbonitrile derivatives as Potent and tissue selective androgen receptor modulators. *J. Med. Chem.* **2014**, *57*, 2462–2471.

(13) Ghali, S. A.; Gottlieb, B.; Lumbroso, R.; Beitel, L. K.; Elhaji, Y.; Wu, J.; Pinsky, L.; Trifiro, M. A. The use of androgen receptor amino/carboxyl-terminal interaction assays to investigate androgen receptor gene mutations in subjects with varying degrees of androgen insensitivity. *J. Clin. Endocrinol. Metab.* **2003**, *88*, 2185–2193.

(14) (a) McComas, C.; Cohen, J.; Huselton, C.; Marella, M.; Melenski, E.; Mugford, C.; Slayden, O.; Winneker, R.; Wrobel, J.; Yudt, M. R.; Fensome, A. Novel progesterone receptor modulators: 4-Aryl-phenylsulfonamides. *Bioorg. Med. Chem. Lett.* **2012**, *22*, 7119–7122. (b) McComas, C.; Fensome, A.; Melenski, E. Cyanopyrrole-phenyl progesterone receptor modulators and uses thereof. U.S. Pat. Appl. Publ. US 20070027125, 2007. (c) McComas, C.; Fensome, A.; Melenski, E. Use of progesterone receptor modulators. U.S. Pat. Appl. Publ. US 20070027201, 2007.

(15) Bohl, C. E.; Miller, D. D.; Chen, J.; Bell, C. E.; Dalton, J. T. Structural basis for accommodation of nonsteroidal ligands in the androgen receptor. *J. Biol. Chem.* **2005**, *280*, 37747–37754.

(16) (a) *Maestro*; Schrödinger, LLC: New York, NY; <http://www.schrodinger.com/>. (b) Halgren, T. A.; Murphy, R. B.; Friesner, R. A.; Beard, H. S.; Frye, L. L.; Pollard, W. T.; Banks, J. L. Glide: A new approach for rapid, accurate docking and scoring. 2. Enrichment factors in database screening. *J. Med. Chem.* **2004**, *47*, 1750–1759.

(17) Winneker, R. C.; Fensome, A.; Zhang, P.; Yudt, M. R.; McComas, C. C.; Unwalla, R. A new generation of progesterone receptor modulators. *Steroids* **2008**, *73*, 689–701.

(18) Williams, S. P.; Sigler, P. B. Atomic structure of progesterone complexed with its receptor. *Nature* **1998**, *393*, 392–396.

(19) (a) Allen, F. H.; Taylor, R. Research applications of the Cambridge Structural Database (CSD). *Chem. Soc. Rev.* **2004**, *33*, 463–475. (b) Allen, F. H. The Cambridge Structural Data Base: a quarter of a million crystal structures and rising. *Acta Crystallogr., Sect.*

B: *Struct. Sci.* **2002**, *58*, 380–388. CCDC Web site database: [http://www.ccdc.cam.ac.uk/free\\_services/website/](http://www.ccdc.cam.ac.uk/free_services/website/).

(20) (a) Pollock, J.; Borkin, D.; Lund, G.; Purohit, T.; Dyguda-Kazimierowicz, E.; Grembecka, J.; Cierpicki, T. Rational design of orthogonal multipolar interactions with fluorine in protein-ligand complexes. *J. Med. Chem.* **2015**, *58*, 7465–7474. (b) Paulini, R.; Miller, K.; Diederich, F. Orthogonal multipolar interactions in structural chemistry and biology. *Angew. Chem., Int. Ed.* **2005**, *44*, 1788–1805.

(21) Perola, E.; Charifson, P. Conformational analysis of drug-like molecules bound to proteins: An Extensive Study of Ligand Reorganization upon Binding. *J. Med. Chem.* **2004**, *47*, 2499–2510.

(22) (a) *Jaguar*, version 9.0; Schrödinger, LLC: New York, NY, 2017. (b) PetaChem, LLC, 26040 Elena Road, Los Altos Hills, CA 94022.

(23) Matsumoto, A. M. Effects of chronic testosterone administration in normal men: safety and efficacy of high dosage testosterone and parallel dose-dependent suppression of luteinizing hormone, follicle-stimulating hormone, and sperm production. *J. Clin. Endocrinol. Metab.* **1990**, *70*, 282–287.